Application of a computer to asymmetric flow measurement in circular pipes

L.A. Salami

Transactions of the Institute of Measurement and Control 1984 6: 197
DOI: 10.1177/014233128400600403

Application of a computer to asymmetric flow measurement in circular pipes

by L. A. Salami, BTech(Mech), PhD, MIMechE, CEng

Experimental investigations into asymmetric flow measurement are usually found to be time consuming and the results generally inconclusive, especially if the error being investigated is within the limits of the accuracy of the ultimate flow measuring device used in the investigation. Therefore, a computer method has been developed in which asymmetric flow measurement has been studied using theoretical velocity profiles. The basic conclusions of the approach have been found to be in agreement with the experimental evidence. Apart from the considerable savings in time, it has also permitted areas in asymmetric flow measurement, which have been hitherto very difficult to investigate experimentally, to be tackled.

Symbols

b Constant to limit radial distance over which the velocity is linear

k Exponent, see general profile functions

m Constant in profile function

n Exponent in velocity power law

Q, Q_{θ° Non-dimensional flowrate; Q_{θ° flowrate along a radius at any angle θ° to a chosen reference radius

$\bar{Q}$ The average flowrate from the 72 equally spaced radii from which the array of radii are chosen

$$\bar{Q} = \frac{1}{72} \sum_{k=0}^{k=71} Q_{\theta^\circ} = 5k$$

Q_{true} Correct flowrate obtained by integrating the velocity profile

$$Q_{\text{true}} = \frac{1}{2} \int_0^{2\pi} \int_0^1 UR \, dR \, d\theta$$

R, $\bar{R}$ Non-dimensional distance using the internal radius of pipe. $\bar{R}$ is $R = 1$

U, $\bar{U}$ Dimensionless velocity at any point using the central velocity; $\bar{U}$ mean dimensionless velocity over the pipe section

U_b Basic velocity profile

U_c Velocity profile that produces asymmetry

y Non-dimensional distance from the pipe wall, i e, $1 - R$

z Constant for changing the inclination of the linear central part of the composite velocity profile relative to pipe axis

θ Orientation of the traversing line to the datum of the profile function

$$\text{Average error } t = \frac{\bar{Q} - Q_{\text{true}}}{Q_{\text{true}}}$$

Glossary

Array of radii:
Arrangement of a given number of radii equally spaced to cover the circular duct, e g, 3, 4, 6 and 8 radii arrays

Array of traversing points:
Arrangement of the total number of traversing points one decides on to traverse a flow, e g, four traversing points/radius for a 6-radii array for an array of 24 traversing points

Error:
The difference between the flowrate given by an array of traversing points and the true flowrate, Q_{true}, expressed as a percentage of the latter

1 Introduction

It is well known that most fluid flows in circular pipes are, in practice, asymmetric. By contrast, the methods of flow measurement given in the National and International Codes, e g, BS 1042 (1943), are usually unsatisfactory because the rules given in these codes are based on the assumption that the flow is almost axi-symmetric. Examples abound in industry in which a flow measurement is required in a plant in which it is virtually impossible to fulfil the latter conditions. Typical examples are: *in-situ* testing of fans and turbines; the air flow measurement in boiler trials; air flow up a chimney stack; and flow measurement downstream of pipe fittings. In some of these, very high accuracy may not be required but in others, eg, fan performance tests, acceptance or rejection will depend on the results obtained for the total efficiency, which, to a large extent, depends on the accuracy with which the flowrate is measured. It is desirable, therefore, to evolve a method of traversing which will ensure reasonable or desired accuracy limits irrespective of the severity of the asymmetry of the flow.

At the instigation of the National Engineering Laboratory, whose flow measurement research programme was being sponsored by the Department of Trade and Industry's Metrology and Standards Requirement Board, an extramural contract was placed with the University of Southampton for a programme of work to be carried out in this field. This programme was to be both experimental and theoretical.

Mechanical Engineering Dept, University of Benin, Benin City, Bendel State, Nigeria.

One way of tackling the above programme is to use the experimental approach. This was reported by the author (Salami, 1975), where about five Velocity-Area Methods were employed with traverse points ranging from 3 to 6 per radius in order to cover all the combinations for the methods considered and the number of points per radius. Traversing took place along 36 radii equally spaced over the pipe-cross-section. It took about two months to investigate a profile completely, principally because of the time consumed in taking the Pitot-tube readings. Data processing was also carried out on a computer to normalise the conditions under which the results were taken, since these varied from hour to hour and from day to day, as well as to correct the velocities given by the Pitot tube used for some of the well known Pitot-static tube errors. It required, therefore, tremendous data collection before any basic conclusions could be drawn from just one profile.

When the results obtained from the experimental approach were compared with those obtained from preliminary work using the computer approach as given by Salami (1971) it was found that many of the conclusions from the two methods were in agreement. Table 1, which gives a comparison between the two approaches, shows that they agree on three major points as follows:

(i) There is little to choose between the velocity–area methods employed. The biggest spread is ± 0.14% for the experimental and ± 0.11% for the theoretical approach.
(ii) The flowrate given by the cubic method was slightly higher than that given by the log–linear and the log–Tchebycheff methods.
(iii) There are some occasions when the average error does not improve with increase in number of points per radius.

Again, both approaches showed that there is a drastic reduction in the maximum error as the number of radii in the array is increased, but that not much reduction occurs between 6- and 8-radii arrays. From the experimental results, for instance, the maximum positive error for the Pitot-static traverse changed from about 1% for the 4-radii array to 0.4% for the 6-radii and to 0.25% for the 8-radii array. For the theoretical profile P6 on the other hand, the corresponding figures are 1.6%, 0.68% and 0.37%, respectively.

The computer method had been introduced basically to simulate the traversing procedure in the computer. The main advantage to be seen with this method was that it could be used to investigate, in a very short time, many aspects of asymmetric flow which would have been time-consuming, and perhaps inconclusive, using the experimental method. Salami (1972) reports on the later work on this project. Another advantage was that it provided theoretically an absolute method of flow measurement which was not possible in the experimental approach especially when air is being used.

TABLE 1: Average error from experimental and theoretical approaches using various velocity-area methods and number of points per radius

	Average error					
	Experimental (Pitot-static)			Theoretical (Profile P6)		
Method	4	5	6	4	5	6
Log–cubic	–0.106	–0.180	–0.116	0.011	0.042	0.009
Cubic	–0.293	–0.165	–0.200	0.112	0.079	–0.040
Log–linear	–0.374	–0.275	–0.230	–0.113	–0.104	–0.070
Log–Tchebycheff	–0.187	–0.242	–0.217	–0.009	–0.074	–0.080

It is these advantages which have prompted more extensive work to be carried out on this computer technique of tackling problems in asymmetric flow measurement, and the main aim of the paper is to explain the method. Towards the end of the paper, the influence of Reynolds number on the accuracy of some velocity-area methods is investigated.

Another aspect investigated is the effect of having to use the wrong value of the exponential in the velocity power law near the wall.

Before leaving this section, however, it is worth emphasising that the computerised method is not meant to replace traversing in practice. Rather, one of its objectives is to aid traversing by pointing out how best to arrange the traverse points so that more accurate results could be obtained. This is so because the method helps to determine the uncertainties introduced by using point measurements.

2 Theoretical velocity profile

Theoretical velocity profiles form the basis of the computer approach. They were evolved as profiles which resembled profiles generally encountered in practice. As it would be difficult, if not impossible, to simulate all the likely profiles which could occur, attempts were made to simulate some of the more common ones. An important requirement was that the velocity should change both along the radius and from one radius to the other, as it does in practice. Another was that the profile function should be capable of being integrated over the cross-section of the circular pipe.

2.1 Theory behind theoretical profiles

For an asymmetric flow in general, the velocity, U, varies from radius to radius on a circle concentric with the pipe centre, i.e. U is a function of the angular position of the radius relative to an arbitrarily chosen datum. No matter how asymmetric a flow may be, it must always have zero velocity at the pipe wall because of the non-slip theory of flow. Consequently, near the wall there must be a laminar layer which will become turbulent as the centre of the pipe is approached. The power law for the velocity distribution must be expected to hold, therefore, for some distance from the wall.

In order to simulate these conditions, the asymmetric velocity profile is assumed to be made up of two components: a basic component, U_b given by the power law

$$U_b = (1 - R)^{1/n} \qquad \ldots(1)$$

and a polynomial component, U_c, superimposed on it and given by

$$U_c = R(1 - R)^{1/k} \qquad \ldots(2)$$

Thus

$$U = U_b + U_c \qquad \ldots(3)$$

U_c vanishes at the centre and the pipe wall, so that the contour for $U = 1$ must pass through the pipe centre.

Moreover, because it contains an exponential, it does not invalidate the assumption that the velocity obeys a power law near the wall.

It is U_c that is used to create the asymmetry of the flow. If it is multiplied by a function, $m \cdot f(\theta)$ where $f(\theta)$ can be any function of θ, different velocity distributions can be obtained. For instance, if $f(\theta)$ is $\sin\theta$ then for half the circle the value of U_c is added to the basic profile, U_b, while for the remaining half the function is subtracted. The severity of the distorted velocity profile obtained can be controlled by the choice of m. The maximum velocity now need no longer occur at the pipe centre as it did for the basic profile.

There are some profiles, however, which are almost flat near the pipe centre, such as flow at the inlet of a pipe from a reservoir, or flows which are only a short distance downstream of an orifice plate in a pipe, etc. These types of flow can be simulated by using a combination of a linear function near the pipe centre and a power law and a polynomial near the wall. Thus, near the centre,

$$U_1 = 1 + zR \sin\theta \qquad \ldots(4)$$

Sin θ is inserted to make the function vary from one radius to the other, as there is hardly a perfectly uniform flow in practice. The value of z changes the inclination of the linear central portion to the pipe axis. At $z = 0$, the profile is perpendicular to the pipe axis. The limit of the central portion is set by $R = b$, where b is an arbitrarily chosen constant between 0 and 1, depending on the type of asymmetry desired.

From the velocity at the limit $R = b$ to the wall at $R = 1$, the velocity is assumed to be made up of the two components U_b and U_c as before, but the exact expression is then modified as follows:

$$U_{b2} = (1 + zb \cdot \sin\theta)\left(\frac{1-R}{1-b}\right)^{1/n} \qquad \ldots(5)$$

and

$$U_{c2} = \frac{m(R-b)(1-R)^{1/k}}{(1-b)^{1/k}} \cdot f(\theta) \qquad \ldots(6)$$

As can be seen from these expressions, $U_{b2} = U_1$ and $U_{c2} = 0$ at $R = b$ so that the magnitude of U does not change as one goes from the inner curve to the outer ones.

It is well known that another way of describing a velocity profile is to use trigonometric functions. This technique has been applied to examine whether it would affect the basic conclusions of this method. In this case the basic profile is now

$$U_b = m \sin\frac{\pi}{2}(1-R)^{1/n} \qquad \ldots(7)$$

while the component that changes the velocity profile to achieve asymmetry is

$$U_c = m \sin\pi(1-R)^{1/k} \cdot f(\theta) \qquad \ldots(8)$$

2.1.1 Radial distribution

From the above it can be seen that three types of function have been used for describing the radial velocity distribution. The first was of the form:

$$U = (1-R)^{1/n} + mR(1-R)^{1/k} f(\theta) \qquad \ldots(9)$$

The shape of this distribution can be changed by varying the values of n, m, k and $f(\theta)$. It was found that this function was quite easy to integrate.

The second type was a composite function of the form:

$$U = 1 + zR \sin\theta \qquad \text{for } R = b \text{ where } 0 = b = 1 \qquad \ldots(10)$$

and

$$U = (1 + zb \sin\theta)\left(\frac{1-R}{1-b}\right)^{1/9} + m\frac{(R-b)(1-R)^{1/k}}{(1-b)^{1/k}} f(\theta)$$

$$\text{for } R = b \qquad \ldots(11)$$

Parameters could be usually chosen so that there is a fairly smooth transition from one type of curve to the other.

The third function used the trigonometric function to describe the velocity profile as follows:

$$U = \sin\frac{\pi}{2}(1-R)^{1/n} + m \sin\pi(1-R)^{1/k} f(\theta) \qquad \ldots(12)$$

The integration of this profile was slightly more complicated than that for the polynomials above, and the procedure for handling it is given in Appendix 1. Again, different velocity profiles can be obtained by n, m, k and $f(\theta)$.

2.1.2 Tangential function

The tangential function $f(\theta)$ allows the velocity to be changed from radius to radius. It was also used sometimes to vary the number of peaks in the velocity contour. However, this function had to be used in conjunction with the other parameters already mentioned above in order to obtain a desired contour.

Various functions which were used were:

$e^{-a\theta} \sin\theta, \sin\theta, \sin^2\theta, (1 - \cos\theta)(\theta^2 - 1),$

$e^{-a\theta} \sin^2\theta, \theta \sin\theta, e^{-a\theta} \sin^2 5\theta, \theta(2-\theta)^2 \sin 3\theta$

The main aim on using many of these functions was simply to ensure that there was nothing abnormal about them and that they did give practical velocity profiles. In choosing the tangential function, steps were taken to ensure that the numerical values of the velocity given by $\theta = 0$ and 2π were the same. It was not always possible to make the tangents at these points the same as well, but it was found from the work carried out at the University of Benin that this was not a very serious disadvantage, since no differentiation was necessary during the investigation.

2.2 Evaluation of exact and average flowrate

A unique feature of the theoretical method is that the functions used are capable of being integrated to give the exact flowrate. This cannot be achieved with the experimental methods. The exact flowrate thus obtained is important, since it serves as an absolute standard against which the errors in any chosen method of traverse can be evaluated.

Since the velocity varies both radially and tangentially, the flowrate will be given by double integration, i e,

$$Q_{\text{true}} = \frac{1}{2\pi}\int_0^{2\pi}\int_0^1 UR \cdot dR \cdot d\theta \qquad \ldots(13)$$

where the symbols carry the usual meanings.

Asymmetric flow measurement is a random event. Consequently, the higher the number of radii over which the transverse takes place, the more accurate should be the result if the average of these results is found. For the purpose of evaluating the average flowrate, $\bar{Q}$, the average of the flowrates given by 72 equally spaced radii could be obtained. Thus

$$\bar{Q} = \frac{1}{72} \sum_{k=0}^{k=71} Q_{\theta^\circ = 5k} \quad \ldots(14)$$

where Q_{θ° is the flowrate along a radius at any angle θ° to the chosen reference radius. The average error, ϵ, is given by

$$\epsilon = \frac{\bar{Q} - Q_{\text{true}}}{Q_{\text{true}}} \quad \ldots(15)$$

2.3 General comments on velocity profiles

In generating the velocity profiles, the parameters were usually arranged so that the maximum velocity occurred between 1.0 and 1.2. This was because in practice it has been found that the maximum velocities very rarely exceed 1.2 of the velocity at the centre of the pipe. In contours which contained a dip it was usually arranged that this did not fall below 0.5 of the velocity at the pipe axis.

The expressions for some velocity–area methods contained the exponent n of the velocity power law:

$$U = (y/R)^{1/n} \quad \ldots(16)$$

Whatever the distribution of the velocity in the central portion of the pipe, this expression is still usually valid near the wall. Hence, the value of n near the wall is quite important. This parameter has therefore been varied either by moving a velocity peak very close to the wall by judicious choice of variables or by making n or k quite prominent.

Altogether, 23 profiles were developed from these components, but it must be stressed that this exercise was by no means exhaustive. Fig 1 shows the 23 profiles developed and although profiles P1–P10 have already been given (in Salami, 1971)they are reproduced for completeness. The equations for the profiles are given in Appendix 2. Exact values of m in some profiles were determined by specifying the maximum value of the velocity U and the radial distance about which it occurs.

2.4 Practical asymmetry flow profile

It is generally not possible in practice to allow for the required number of pipe lengths between an obstruction such as a pipe fitting and the traverse plane. The type of asymmetric flow distribution produced depends on how far the traverse plane is downstream of the obstruction. Common pipe fittings which cause asymmetric flows are bends, valves and orifices. Although there are some data on velocity distribution downstream of a bend, eg, Murakami & Shimizo, 1978 and Akaike *et al*, 1978, and orifice plates, Akaike *et al*, 1978, there is very little for partly opened valves or heat exchangers.

Some of the velocity distributions given here, eg, P4, P8, P11, P12 and P14, are quite similar to velocity profiles after bends; P3 is similar to velocity profiles 6 to 16 diameters downstream of an orifice plate, while P6, P9, P17 and P19 resemble the experimental flow profile investigated in Salami (1975) which was obtained by making an eccentric hole in a closed-mesh wire gauze placed in the pipe.

Multi-peak profiles such as P5, P10, P16, P20, P21, P22 and P23 were inserted for two reasons. First, they simulated conditions after some circular heat exchangers and in chimney stacks, and second they ensured that the peaks were not along regular positions, e g, diametrically opposite each other, etc.

3 Velocity – area methods

Several well known velocity–area methods were assessed in this study. These included the Log–linear, Simpson's Rule, Cubic, Tangential, AMCA, and Log–Tchebycheff. After the work by Salami (1971), the Tangential and the Simpson's Rule methods were dropped because they were always giving very poor results. For the remaining velocity–area methods, the theory behind their derivation and the location of the traversing points, once the number is given, can be found in the following references: Log–linear – Winternitz & Fischl, 1957; Method of Cubics – ISO, 1969; AMCA – ISO, 1970; and Log–Tchebycheff – Winternitz & Fischl, 1957. These methods, together with the new one suggested below by the author and called Log–cubics, were used in the analytical investigation.

3.1 Log–cubic method

At an early stage of this work it was found that the differences between the various velocity–area methods were relatively small; none of the four remaining ones being assessed was giving the best result consistently, neither was the margin between them very substantial. For instance, as already pointed out, the variation in the average error was within ±0.12%. Compared with the average difference between the 4- and 6-radii arrays which is about 1.36% and that for the 4- and 8-radii of about 1.40%, this difference is quite trivial. Consequently, it could be concluded that there was not much to be gained by developing yet another velocity–area method. It was noticed, however, that the log–linear method always tended to underestimate the flow, while the Cubic method generally tended to overestimate the flow. This prompted the idea of using the log–linear point locations in the method of Cubics and so a special 'hybrid' method was evolved which would become known as Log–cubic.

4 Computer program

The computer program simulates the Pitot traverse procedure. Arrays of traversing points are chosen, and the flowrate obtained is compared with that obtained from the exact integration of the profile function. A set of results is obtained by choosing the array of radii from 72 equally spaced radii over the cross-section of the pipe. The average error and the standard deviation of the set are calculated. While the actual program used can be found in Salami, 1972, a flow chart is given in Fig 2 showing the major steps. The functions of the various parts of the program are as follows:

4.1 Main program

After choosing a particular velocity–area method, the program computes the radial disposition of the

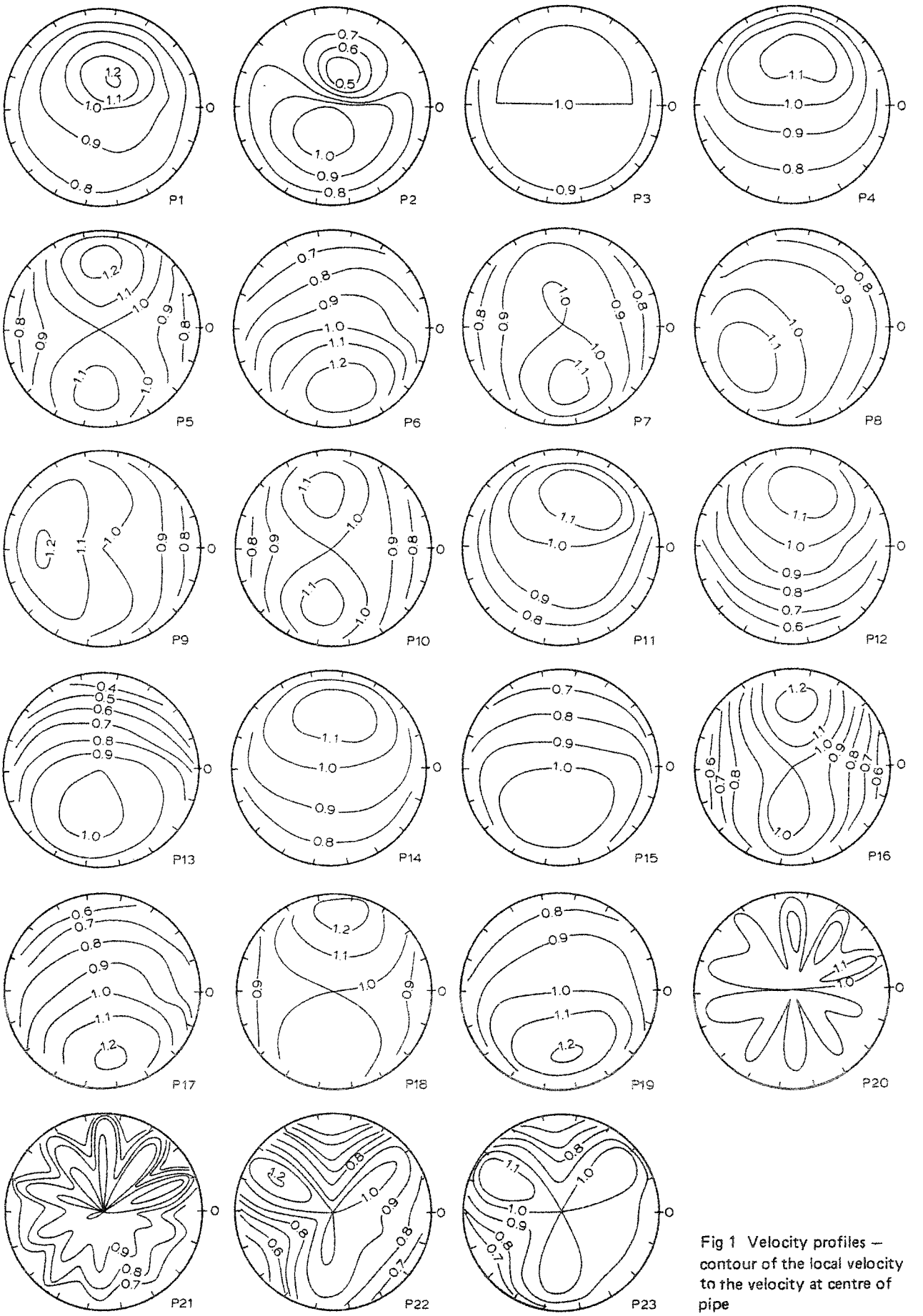

Fig 1 Velocity profiles — contour of the local velocity to the velocity at centre of pipe

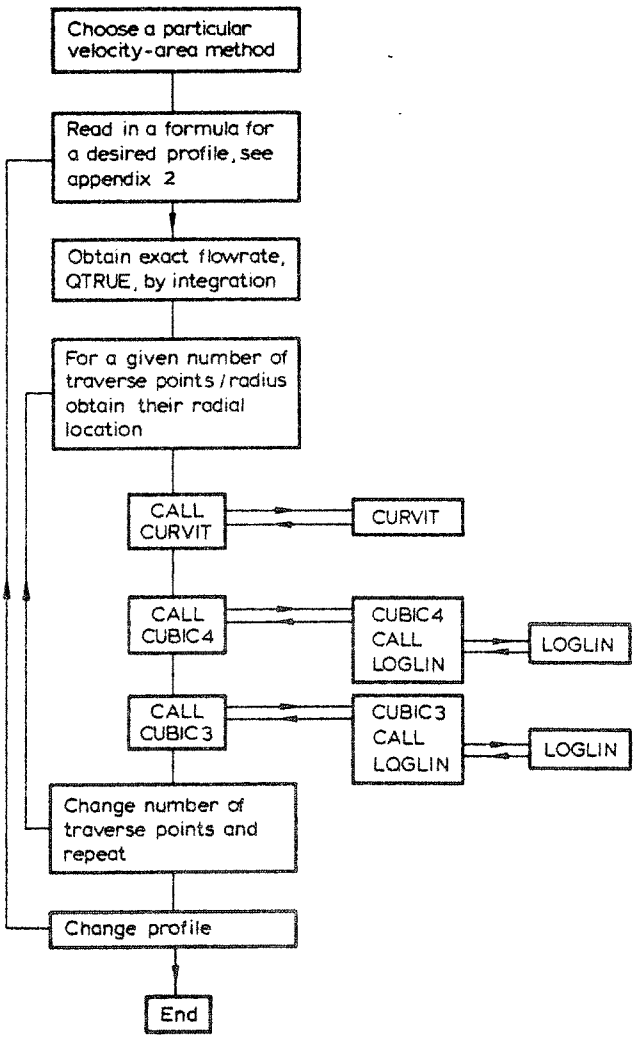

Fig 2 Flow chart of the computer program

traverse points for the number of traverse points per radius desired. The correct flowrate, Q_{true}, is evaluated, and it is against this that all other flowrates obtained from different arrays are compared, to calculate the error.

4.2 Subroutine CUVFIT

There are some velocity–area methods, e g, Cubic method, which require the value of the exponent of the velocity power law near the wall to be selected for the computation of the flowrate. This subroutine fits an exponential curve between the last traverse point and the wall and obtains the value of the exponent and stores them for the 72 radial positions.

4.3 Subroutine CUBIC4

This subroutine performs several functions using 4- and 8-radii arrays. These include

(a) Calls Subroutine LOGLIN
(b) Combines the velocities on the array of radii of 4 and 8 and finds the average velocity
(c) Computes the flowrate and compares it with Q_{true} and obtains the relative error
(d) After obtaining the relative errors for a complete set of results, computes the average error and the standard deviation of the set.

4.4 Subroutine CUBIC3

This subroutine performs the same functions as CUBIC4 above, but uses 3- and 6-radii arrays instead of 4- and 8-radii arrays.

4.5 Subroutine LOGLIN

This subroutine computes the velocity at every traverse point and adds them up in a manner dictated by the velocity–area method under consideration.

5 Discussion

Asymmetric flow traversing is a random event, and as such, recommendations from the investigation carried out in this study are best made on the basis of statistical analysis rather than on a particular set of results. This analysis formed part of the work reported in Salami, 1972a. Here discussion will be concentrated on the influence of various important factors on the theoretical accuracy to be expected from the computer approach.

5.1 Effect of using sine function instead of polynomials

No significant difference was noticed when sine functions were used instead of polynomials in describing the radial distribution of velocity. However, the integration was more involved than with the polynomial, (see Appendix 1), and included the raising of π to high powers. This necessitated the use of DOUBLE PRECISION in parts of the computer program in order to obtain good results and may, therefore, increase the computer time slightly.

5.2 Log–cubic method

Table 2 shows the number of times each of the methods written above each column is better than any of the other methods considered, using the average error and the maximum error as criteria. The combined results of 4, 5 and 6 points per radius for each of the 23 velocity profiles (which give a total of 69), have been used for the comparison.

A velocity–area method which has the lowest average error shows that if a very large set of results is taken, this method gives the best result. On the other hand, a method which gives the lowest maximum error indicates that if a

TABLE 2: Number of times the velocity–area method given above the column is best when compared with other methods using the Average Error and Maximum Error as the criteria

	Log–cubic	Cubic	Log–linear	Log–Tchebycheff
	Average error			
	17	37	8	7
No. of radii in array	Maximum error			
4	34	14	11	10
6	31	18	12	8
8	26	24	12	7

single result were taken and it happened to be at the position that gave the poorest result, that method gives the best.

By having a closer look at Table 2, it can be seen that no velocity–area method is consistently better than others, whichever criterion is used. There is always a combination of circumstances which can make one method better than others.

Based on average error, the Cubic method is the best. However, if comparison is on the basis of maximum error, then the Log–cubic method is best. It can generally be concluded that on the whole the Log–cubic is slightly the better.

Unfortunately, the Log–cubic method was found to combine most of the separate disadvantages of the Log–linear and the Cubic methods. Thus, it has the disadvantage of being sensitive to whether the number of traverse points per radius is odd or even and is also inflexible as far as the location of the traverse points is concerned, once their number per radius has been decided. Moreover, it inherits from the method of Cubics the disadvantages of cumbersome arithmetic and the fact that the accuracy is influenced by the value of the exponent used.

5.3 Effect of changing the value of the exponent *n*

There were a few profiles where the average value of the exponent *n* was about 9, eg, profiles P1–P10. This corresponds to a Reynolds number of nearly 10^6 in a long pipeline. In many practical applications the exponent may not be as high as this, first because the flowrate itself may not be high, and second the pipe wall could be rough. Consequently, it was thought to be useful to see what effects lower values of *n*, eg, 5 or 7, would have in the

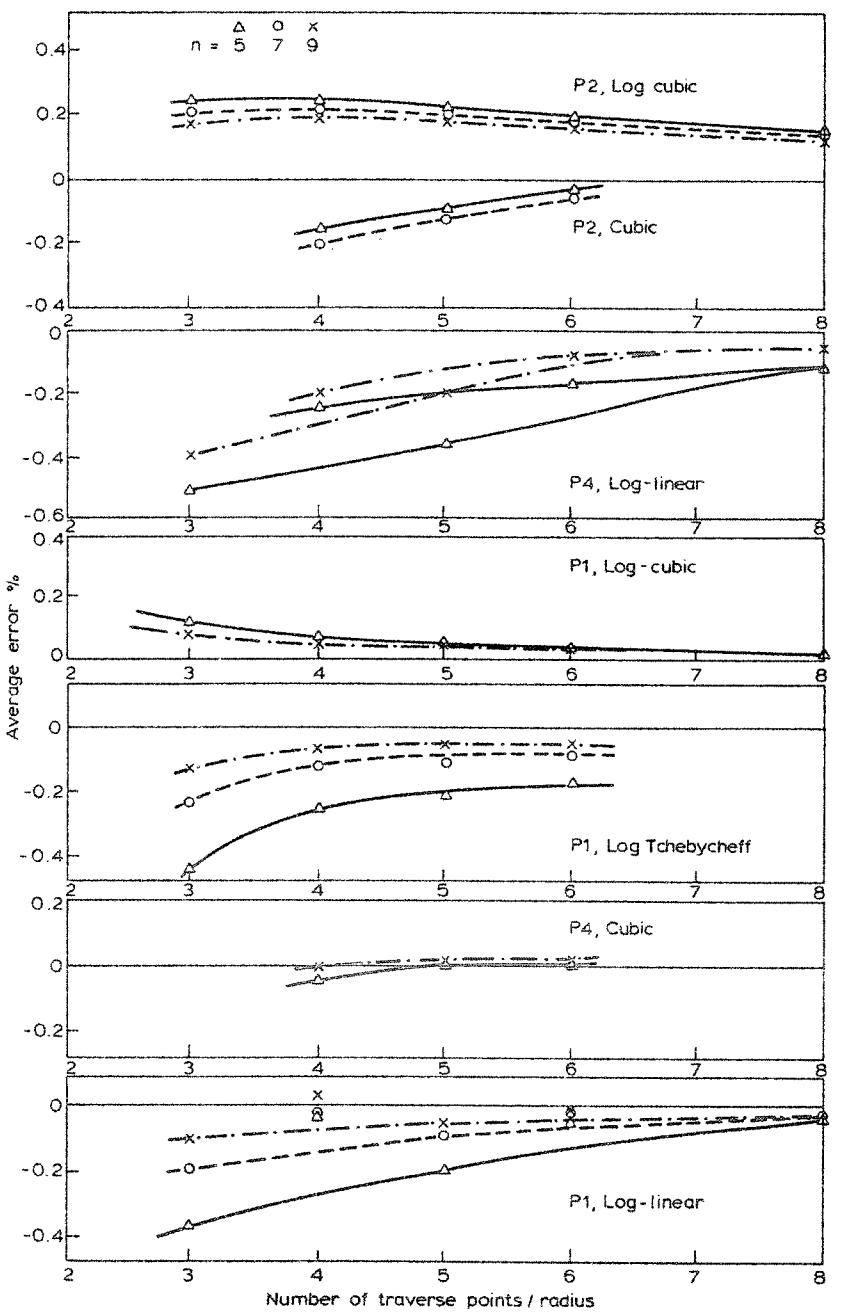

Fig 3 Effect of using other values of the exponent *n* — three values of *n* used in the profile functions instead of *n* = 9 in profiles P1–P10

profile function. The investigation was carried out and the results are shown in Fig 3.

Broadly, the result for the Log–linear and Log–Tchebycheff was found to be quite sensitive to this effect and usually showed some improvement as n increased. On the other hand, the results for both the Log–cubic and the Cubic methods were virtually insensitive to changes in this quantity. Since at high Reynolds number the Log–linear and the Log–Tchebycheff methods do not show any particular superiority over the Log–cubic and Cubic methods, the latter two may prove even more accurate than the former two at lower Reynolds numbers.

It should be pointed out, however, that by changing the value of n the profile is also changed. The reason for the general improvement in the results from the Log–linear and Log–Tchebycheff methods with increasing values of n could be due to the fact that the profiles are approaching more and more closely those on which the assumptions for the method are based. For the Log–cubic and the Cubic methods on the other hand, the value of n is incorporated, and therefore the methods do allow for any changes.

5.4 Effect of using wrong exponent

In many practical applications it would be difficult and time-consuming to obtain the extra points between the last traverse point and the wall in order to calculate the value of n to be employed in those velocity–area methods which require it, e g, Cubic and Log–cubic. The exponent may therefore, have to be guessed. It would be useful to know the magnitude of the error to be expected if the wrong value of n has to be used in the formula.

Fig 4 shows the effects on the Log–cubic and the Cubic methods respectively of using other values of n different from the correct mean value of 9 used in profiles P1–P10. For the Log–cubic method there is only a slight discrepancy when 3 and 5 points per radius are used for the range of exponent 3–11 considered. The same conclusion applies to the Cubic method with 6 points per radius. On the other hand, the discrepancy is quite substantial, especially at low values of n for the Log–cubic method with 4 and 6 points and the Cubic with 4 and 5 points.

Apart from the unpredictable behaviour of the Log–cubic method due to even and odd numbers of traverse points, the error due to using the wrong exponent generally diminishes with increase in the number of traverse points per radius. The error can be fairly large for a small range of uncertainty; e g, for the method of Cubics there is a discrepancy of 0.2% in the average error due to using $n = 8$ instead of $n = 9$ for 4 traverse points per radius. The improvement in the discrepancy due to using the wrong value of n with the number of traverse points per radius noted above is partially due to the reduction in the region near the wall which is affected by the value of n.

6 Conclusion

With the aid of theoretical velocity profiles and computer programs it has been demonstrated that asymmetric flow traversing can be simulated. Previous experimental investigations have confirmed good agreement between this new approach and the experimental method. The computer method, therefore, offers a speedy and economical aid to studying asymmetric flows. An attempt has been made here to make the theoretical velocity profile as realistic as possible and to cover quite a range of possibilities in this field.

The investigations carried out have demonstrated that, provided one of the four methods studied here is employed, the difference in the result is relatively trivial and therefore, the choice of the velocity–area method is not a major source of error in asymmetric flow measurement. Consequently, no radically new velocity–area method is being proposed. However, the Log–cubic method which was evolved as a combination of the Log–linear and the Cubic methods is presented. Although the method was found to be slightly better than other methods, it was not consistently so, and it suffered from the disadvantages of both the Log–linear and the Cubic methods. Its use may therefore be limited.

Some asymmetric flow problems, e g, the effect of having to guess the value of n, the exponent in the velocity power law near the wall, have been tackled. They would have been difficult to investigate experimentally and even then, the results could have been inconclusive. Therefore, the conclusions from these analyses are valuable.

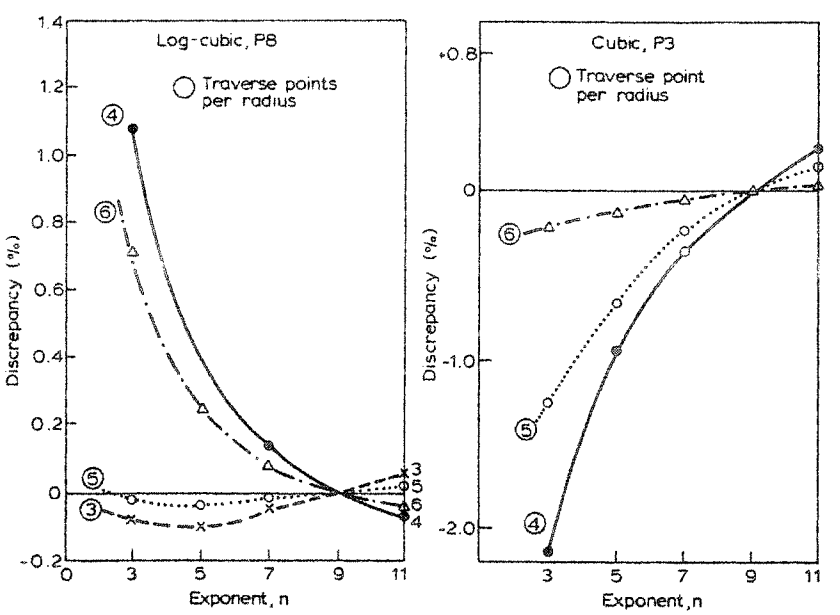

Fig 4 Discrepancy due to using the wrong values of the exponent n in the Log–cubic and the Cubic methods for various traverse points per radius

7 Acknowledgement

The author is very grateful to Prof S. P. Hutton who supervised the project at the University of Southampton. His gratitude also goes to Dr E. A. Spencer and Dr F. C. Kinghorn, both of National Engineering Laboratory (NEL), East Kilbride, Glasgow, for their interest in the work. Funds for the original research was provided by the Department of Trade and Industry and the work developed at the University of Southampton; the author is very thankful to them.

References

Akaike, S., Toyokura, T., Sugiyama, S. and Amemori, H. 1978. 'Study of flow straightening of turbine flowmeter', *Bulletin JSME*, 21 (157), 1152–1159.

British Standards BS 1042 1943 Part 2: 'Methods of the measurement of Fluid Flow in Pipes'.

ISO Technical Committee. 1969. *Rapport de la délégation Française sur la méthode de calculi du debit-volume* ISO/TC 30/GT (France-3) 14F.

ISO Technical Committee. 1970. *Remerque du comité membre Français sur le document ISO/TC 30/GT 8 (Secr. 11) 26,* ISO/TC 30/GT 8 (France 6) 29F.

Murakami, M. and Shimizo, Y. 1978. 'Asymmetric Swirling Flows in Composite pipe bends', *Bulletin, JSME,* 21, (157), 1144–1151.

Salami, L. A. 1975. 'Experimental investigation into errors in the velocity–area methods of measuring asymmetric flows in circular pipes' *Conference on Fluid Flow Measurement in the Mid 1970's,* National Engineering Laboratory, East Kilbride, Glasgow, UK, Paper G-3.

Salami, L. A. 1971. *Error in the velocity–area methods of measuring asymmetric flows in circular pipes.* Modern Developments in Flow Measurement, Peter Peregrinus Ltd, 381–400.

Salami, L. A. 1972. 'On velocity–area methods for asymmetric profiles'. *Interim Report No. V, University of Southampton Report No ME/72/55.*

Salami, L. A. 1972a. 'On velocity–area method for asymmetric profiles – Statistical analysis of 23 theoretical profiles'. *Interim Report No VI, University of Southampton Report No ME/72/56.*

Winternitz, F. A. L. and Fischl, C. F. 1957. 'A simplified integration technique for pipe flow measurement', *Water Power*, June, p. 225.

APPENDIX 1

Integration of profile with sine function

For these profiles

$$U = \sin\frac{\pi}{2}(1-R)^{1/n} + m\sin\pi(1-R)^{1/k} f(\theta)$$

Now

$$Q = \int_0^{2\pi}\int_0^1 U\,R\,dR\,d\theta$$

$$\therefore Q = \int_0^{2\pi}\int_0^1 \{[\sin(\pi/2)(1-R)^{1/n} + m\sin\pi(1-R)^{1/k} f(\theta)]\} \times R\,dR\,d\theta \quad \ldots(A1)$$

Let

$$x = (1-R)^{1/n}$$

$$\therefore 1 - x^n = R$$

$$-nx^{n-1}\,dx = dR$$

Similarly let

$$y = (1-R)^{1/k}$$

$$\therefore 1 - y^k = R$$

$$\therefore -ny^{k-1}dy = dR$$

Thus Eqn (A1) becomes

$$Q = \int_0^{2\pi}\int_0^1 -nx^{n-1}(1-x^n)\sin(\pi/2)\,x\,dx\,d\theta + \int_0^{2\pi}\int_0^1 -ky^{k-1}(1-y^k)\sin\pi\,y\,dy\,f(\theta)\,d\theta$$

$$\therefore Q = -2\pi\int_0^1 nx^{n-1}\sin(\pi/2)\,x\,dx + 2\pi\int_0^1 nx^{2n-1}\sin(\pi/2)\,x\,dx + \int_0^{2\pi} f(\theta)\,d\theta \times\left\{\int_0^1 k\,y^{k-1}\sin\pi\,y\,dy - \int_0^1 k\,y^{2k-1}\sin\pi\,y\,dy\right\} \quad \ldots(A2)$$

$$= -2\pi\cdot\mathrm{SUM1} + 2\pi\cdot\mathrm{SUM2} + F(\theta)(\mathrm{SUM3} - \mathrm{SUM4}) \quad \ldots(A3)$$

where SUM1, SUM2, SUM3 and SUM4 are the integrands in Eqn (A2) in the order in which they appear and

$$F(\theta) \text{ is } \int_0^{2\pi} f(\theta)\,d\theta.$$

If $Q = \bar{U}\pi\bar{R}^2 = \pi\bar{U}$ where $\bar{U}$ is the mean velocity (non-dimensional) across the pipe section and $\bar{R} = 1$.

$$\therefore \bar{U} = Q_{\text{true}} = 2(\mathrm{SUM2} - \mathrm{SUM1}) + \frac{F(\theta)}{\pi}(\mathrm{SUM3} - \mathrm{SUM4})$$

This shows the derivation of Q_{true} used in the computer programs.

The integrands SUM1, SUM2, SUM3 and SUM4 are obtained by partial integration and the program is written so that Q_{true} can be found once n and k are given. They are given below:

$$\begin{aligned}\mathrm{SUM1} = {} & n(2/\pi)\cos(\pi/2)\,x\cdot x^{n-1} \\ & - n(n-1)(2/\pi)^2\sin(\pi/2)\,x\cdot x^{n-2} \\ & - n(n-1)(n-2)(2/\pi)^3\cos(\pi/2)\,x\cdot x^{n-3} \\ & - n(n-1)(n-2)(n-3)(2/\pi)^4\sin(\pi/2)\,x\cdot x^{n-4} \\ & + n(n-1)(n-2)(n-3)(n-4)(2/\pi)^5 \\ & \times\cos(\pi/2)\,x\cdot x^{n-5} \\ & - n(n-1)(n-2)(n-3)(n-4)(n-5)(2/\pi)^6 \\ & \times\sin(\pi/2)\,x\cdot x^{n-6} \\ & + \ldots\end{aligned}$$

$$\begin{aligned}\text{SUM2} = {} & n(2/\pi)\cos(\pi/2)\,x\cdot x^{2n-1} \\ & -n(2n-1)(2/\pi)^2\sin(\pi/2)\,x\cdot x^{2n-2} \\ & +n(2n-1)(2n-2)(2/\pi)^3\cos(\pi/2)\,x\cdot x^{2n-3} \\ & +n(2n-1)(2n-2)(2n-3)(2/\pi)^4 \\ & \times \sin(\pi/2)\,x\cdot x^{2n-4} \\ & -n(2n-1)(2n-2)(2n-3)(2n-4)(2/\pi)^5 \\ & \times \cos(\pi/2)\,x\cdot x^{2n-5} \\ & -n(2n-1)(2n-2)(2n-3)(2n-4)(2n-5) \\ & \times (2/\pi)^6\sin(\pi/2)\,x\cdot x^{2n-6} \\ & +\ldots\end{aligned}$$

$$\begin{aligned}\text{SUM3} = {} & k(1/\pi)\cos\pi y\cdot y^{k-1} \\ & -k(k-1)(1/\pi)^2\sin\pi y\cdot y^{k-2} \\ & -k(k-1)(k-2)(1/\pi)\cos\pi y\cdot y^{k-3} \\ & +k(k-1)(k-2)(k-3)(1/\pi)^4\sin\pi y\cdot y^{k-4} \\ & +k(k-1)(k-2)(k-3)(k-4)(1/\pi)^5 \\ & \times \cos\pi y\cdot y^{k-5} \\ & -k(k-1)(k-2)(k-3)(k-4)(k-5)(1/\pi)^6 \\ & \times \sin\pi y\cdot y^{k-6} \\ & +\ldots\end{aligned}$$

$$\begin{aligned}\text{SUM4} = {} & k(1/\pi)\cos\pi y\cdot y^{2k-1} \\ & -k(2k-1)(1/\pi)^2\sin\pi y\cdot y^{2k-2} \\ & -k(2k-1)(2k-2)(1/\pi)^3\cos\pi y\cdot y^{2k-3} \\ & +k(2k-1)(2k-2)(2k-3)(1/\pi)^4\sin\pi y\cdot y^{2k-4} \\ & +k(2k-1)(2k-2)(2k-3)(2k-4)(1/\pi)^5 \\ & \times \cos\pi y\cdot y^{2k-5} \\ & -k(2k-1)(2k-2)(2k-3)(2k-4)(2k-5) \\ & \times (1/\pi)^6\sin\pi y\cdot y^{2k-6} \\ & +\ldots\end{aligned}$$

It can be seen that the coefficient of the above terms could be quite large when n or k is above 4. Also, π has to be raised to high powers. Consequently, some of the variables in the program for evaluating Q_{true} are in DOUBLE PRECISION which allows the computer to use 20 digits for these variables instead of the usual 10.

APPENDIX 2

Formulae for velocity profile functions

P1 $U=(1-R)^{1/9}+mR(1-R)^2e^{-0.5\theta}\sin\theta$

(m is decided by the condition that $U_{\max}=1.18$ at $R=1/3$)

P2 $U=(1-R)^{1/9}-mR(1-R)^2e^{-0.5\theta}\sin\theta$

(m is decided by the condition that $U_{\min}=0.5$ when $R=1/3$)

P3 $U=1-0.02R\sin\theta$

for $R\leqslant b$ where $b=0.731707$

$$U=(1-0.02b\sin\theta)\left(\frac{1-R}{1-b}\right)^{1/9}+\frac{(R-b)(1-R)^2}{(1-b)^2}$$

$\times e^{-0.5\theta}\sin\theta$ for $R>b$

P4 $U1-\dfrac{0.12}{b}R\sin\theta$ for $R\leqslant b$ where $b=0.343903$

$$U=(1-0.12\sin\theta)\left(\frac{1-R}{1-b}\right)^{1/9}+2\frac{(R-b)(1-R)^2}{(1-b)^2}$$

$\times e^{-0.5\theta}\sin\theta$

P5 $U=(1-R)^{1/9}+mR(1-R)^{1/9}e^{-0.1\theta}\sin^2\theta$

(m is decided by the condition that $U_{\max}=1.10$ when $R=0.9$)

P6 $U=(1-R)^{1/9}+\dfrac{0.5}{\pi}R(1-R)^{1/4}\sin\theta$

P7 $U=(1-R)^{1/9}+\dfrac{1}{\pi^2}(1-R)^{1/4}(1-\cos^2\theta)$

P8 $U=(1-R)^{1/9}+\dfrac{0.04}{\pi}(1-R)^{1/4}(\theta^2-1)(1-\cos\theta)^2$

P9 $U=(1-R)^{1/9}+\dfrac{2}{\pi^5}(1-R)^{1/4}R\theta^2(2\pi-\theta)^2$

P10 $U=(1-R)^{1/9}+\dfrac{2}{\pi^3}R(1-R)^{1/4}(2\pi-\theta)\sin^2\theta$

P11 $U=\sin\dfrac{\pi}{2}(1-R)^{1/4}+0.05\sin\pi(1-R)^{1/2}e^{-0.5\theta}\sin\theta$

P12 $U=(1-R)^{1/7}+R(1-R)^{1/9}e^{(0.05\pi-0.2\theta)}\sin\theta$

P13 $U=(1-R)^{1/7}-R(1-R)^{1/9}e^{(0.05\pi-0.2\theta)}\sin\theta$

P14 $U=\sin\dfrac{\pi}{2}(1-R)^{1/5}+\sin\pi(1-R)^{1/2}0.3\,e^{-0.2\theta}\sin\theta$

P15 $U=\sin\dfrac{\pi}{2}(1-R)^{1/5}-\sin\pi(1-R)^{1/2}0.3e^{-0.2\theta}\sin\theta$

P16 $U=(1-R)^{1/7}+0.05\pi R(1-R)^{1/9}e^{-0.2\theta}\sin^2\theta$

P17 $U=(1-R)^{1/7}-\dfrac{0.4}{\pi}R(1-R)^{1/9}\theta\sin\theta$

P18 $U=\sin\dfrac{\pi}{2}(1-R)^{1/5}+0.6\sin\pi(1-R)^{1/5}e^{-0.2\theta}\sin^2\theta$

P19 $U=\sin\dfrac{\pi}{2}(1-R)^{1/5}-\dfrac{0.175}{\pi}\sin(1-R)^{1/2}\theta\sin\theta$

P20 $U=(1-R)^{1/4}+R(1-R)^{1/9}e^{(0.075\pi-0.3\theta)}\sin^2 5\theta$

P21 $U=\sin\dfrac{\pi}{2}(1-R)^{1/7}+\sin\pi(1-R)^{1/2}e^{(0.025\pi-0.3\theta)}\sin^2 5\theta$

P22 $U=(1-R)^{1/7}+\dfrac{1}{6}\pi^2(1-R)^{1/9}(2\pi-\theta)^2\theta\sin 3\theta$

P23 $U=\sin\dfrac{\pi}{2}(1-R)^{1/5}+\dfrac{\pi^2}{12}\sin\pi(1-R)^{1/3}(2\pi-\theta)^2\theta\sin 3\theta$